The Concept of a Microwave Radar with an Asymmetric Knifelike Beam for the Remote Sensing of Ocean Waves

V. YU. KARAEV, M. B. KANEVSKY, AND G. N. BALANDINA

Institute of Applied Physics, Russian Academy of Sciences, Nizhny Novgorod, Russia

P. CHALLENOR, C. GOMMENGINGER, AND M. SROKOSZ

Southampton Oceanography Centre, Southampton, United Kingdom

(Manuscript received 2 December 2004, in final form 10 April 2005)

ABSTRACT

The features of near-nadir probing of the ocean surface from a satellite are investigated, and a new configuration of a microwave radar for the surface slopes measurement is proposed. Numerical modeling is used to examine the feasibility of a spaceborne implementation, to devise a measuring technique, and to develop a data processing algorithm.

It is shown that the radar with a knifelike beam (1° × 25°–30°) can be used to measure the variance of surface wave slopes. Using range selection and a new processing procedure to synthesize data, it is possible to achieve the spatial resolution required to study wave processes on the ocean surface from satellites. A new approach to wind speed retrieval at and near nadir is also discussed.

1. Introduction

Remote sensing is widely used for oceanographic research. At present, spaceborne radars allow us to obtain a global overview of the ocean surface state and to obtain information on its characteristics, for example, significant wave height (altimeter), wind speed (altimeter and scatterometer), wind direction (scatterometer), and sea wave spectrum [synthetic aperture radar (SAR)]. This information is useful for a wide range of applications in oceanography, meteorology, and navigation.

For active microwave radars, all retrieval algorithms are based on the fact that the electromagnetic waves scattered by the ocean surface contain information about its characteristics. Therefore, the problem of the retrieval of useful information from the ocean surface includes two stages. First, we must determine the optimum radar parameters and which characteristics of the reflected signal we need to recover. Existing publications make it clear that modern radar systems have shortcomings, and new radars are constantly being developed (e.g., Lin et al. 2000; Moccia et al. 2000; Hauser et al. 2001). These new systems aim to measure ocean parameters more precisely or to obtain data across a wider swath to improve sampling. Second, in contrast to buoys, radars cannot directly measure the characteristics of the sea surface. Therefore, it is important to develop good data processing and retrieval algorithms.

An altimeter is one of most advanced tools among modern radar systems for remote sensing due to its capabilities. One may measure the level of the ocean (and then derive an estimate of surface geostrophic currents), the significant wave height, and the wind speed (from backscattered power). The precision of retrieved wind speed may be further improved by using sea state data, and new retrieval algorithms are an active area of research (see, e.g., Gourrion et al. 2000; Gommenginger et al. 2002).

Our earlier investigations (Karaev et al. 1999, 2002b) show that there is a basic limit for the precision of wind speed retrieval from altimeter data because of the complicated correlation between wind speed and radar cross section (RCS). The development of new two-parameter algorithms using both radar cross section and significant wave height permits us to improve marginally the precision of wind speed retrieval in compari-

Corresponding author address: V. Karaev, Institute of Applied Physics, Russian Academy of Sciences, 46, Uljanov str., Nizhny Novgorod, Russia.
E-mail: volody@hydro.appl.sci-nnov.ru

son to one-parameter algorithms. However, it is clear that there is still room for improvement. At nadir, the radar cross section depends on the effective reflection coefficient (i.e., local wind speed) and the variance of sea surface wave slopes (i.e., local wind speed and swell) (Karaev et al. 2002a; Bass and Fuks 1972; Valenzuela 1978). Modern spaceborne radar systems do not measure surface wave slopes, and this uncertainty leads to errors in wind speed retrieval by existing algorithms.

The purpose of the present research is to increase the number of characteristics of the ocean surface that can be measured by microwave radars at and near nadir, and to show the way to improve the precision of wind speed retrieval. Section 1 describes the fundamental assumptions that are used. Section 2 presents the methods for measuring large-scale wave slopes and wind speed by a radar with an asymmetric knifelike beam. In section 3 the spatial resolution problem for such a satellite-borne radar is discussed. Section 4 contains a brief description of a new model for the Doppler spectrum of such a system. Section 5 gives details of the special synthesis procedure used for data processing. In section 6, numerical simulations are used to illustrate the features of the new radar, and section 7 gives an example of data processing.

2. Initial assumptions

As is well known, at small incidence angles, microwave backscatter from the ocean is quasi-specular and takes place from the facets of the ocean surface oriented perpendicularly to the incident electromagnetic wave (Bass and Fuks 1972; Valenzuela 1978). Therefore, it is well recognized that the radar cross section depends on the variance of the slopes of large-scale waves and on the spectral density of the small ripples responsible for the diffuse scattering.

Here we will analyze the properties of microwave signal scattered by sea surface. Namely, centimeter waves (1–10 cm) contain the maximum information about the state of a near-surface layer.

In the framework of the Kirchoff approximation, which does not account for radar frequency dependence, a theoretical analysis of the backscattering of electromagnetic waves from the ocean surface at normal incidence has been carried out for a wide radar beam, and a new theoretical model of the normalized radar cross section (NRCS) has been obtained (Karaev and Kanevsky 1999; Karaev et al. 2002b):

$$\sigma_0 = \frac{|R_{\mathrm{eff}}(U_{10})|^2}{2}\left(S_{xx}^2 + \frac{\delta_x^2}{5.52}\right)^{-1/2}\left(S_{yy}^2 + \frac{\delta_y^2}{5.52}\right)^{-1/2}, \tag{1}$$

where δ_x, δ_y are the half-power beamwidths in two mutually perpendicular planes, S_{xx}^2 and S_{yy}^2 are the variances of surface slopes along and perpendicular to the footprint's major axis, and U_{10} is the wind speed at 10-m height. The antenna gain is assumed to be a Gaussian function. The effective reflection coefficient $R_{\mathrm{eff}}(U_{10})$ is introduced instead of the Fresnel coefficient. This coefficient takes into account the diffuse scattering of the reflected field due to the small-scale waves. Hence, the radar cross section depends on both large-scale waves and little ripples.

In the general case of mixed sea (wind waves plus swell) the characteristics of large-scale waves do not correlate strongly with local wind speed. Only the wind waves depend on the local wind speed. The presence of swell makes the connection between the wind speed and large-scale waves less strong [this is particularly true for significant wave height (SWH), although a little less critical for slopes]. At low wind speed (<6 m s^{-1}), swell may increase the variance of surface slopes two- or threefold (Hwang and Shemdin 1988).

The correlation between short waves and wind speed is strong, and it is demonstrated by the short time relaxation for ripples when wind stress suddenly disappears. On the other hand, NRCS depends on the variance of large-scale waves. As a result, the connection between the reflected power and wind speed is ambiguous, and this is one of the reasons for errors in one- and two-parameter retrieval algorithms.

The direct measurement of the variance of surface wave slopes by radar would permit us to take these into account and make the connection between NRCS and wind speed less ambiguous. Therefore, the measurement of surface wave slopes would allow us to improve the precision of the wind speed retrieval in comparison to the present situation where two variables [see Eq. (1)] are unknown (long-wave slopes and wind speed). Also, we should note that the radar will measure slopes that differ significantly from those measured by buoys. A buoy cannot measure sea waves shorter than ~10 m, while the new radar will measure the slopes of waves shorter than 1 m (Bass and Fuks 1972; Karaev et al. 2002b).

Of course, there are already methods for measuring wave slopes from aircraft (see, e.g., Walsh et al. 1985; Walsh and Vandemark 1998; Hauser et al. 1992). These are provided by good spatial resolution achievable with radars mounted on aircraft. Such radars can see a cell less than 0.3 m × 0.3 m. Special algorithms allow the retrieval of detailed information about the ocean surface, but this approach is too complicated for use from a satellite. Here we suggest another approach to this problem.

At small incidence angles the radar cross section depends on the variance of long-wave slopes. An increase in incidence angle leads to a decrease in normalized radar cross section due to a reduction in the number of perpendicularly oriented facets. At nadir, the NRCS is described by the well-known formula for the narrow radar beam (i.e., for the incident plane wave) (Bass and Fuks 1972; Barrick 1972; Valenzuela 1978):

$$\sigma_{00} = \frac{|R_{\rm eff}(U_{10})|^2}{2S_{xx}S_{yy}}. \tag{2}$$

It can be seen from Eq. (2) that, in this case, the radar cross section does not depend on the characteristics of the antenna system for a narrow radar beam.

3. The measurement of the variance of long-wave slopes by knife-beam radar

Our previous investigations (Karaev and Kanevsky 1998, 1999) show that using a radar with an asymmetric knifelike beam aligned with the direction of flight allows the measurement of the variance of surface wave slopes along the direction of flight. Fortunately, the result does not depend on the height of flight, and, what is more, an increase in height of the sensor above the sea surface leads to a reduction of the fluctuations in the reflected signal due to a larger scattering footprint.

Let us suppose that the parameter δ_x in Eq. (1) is small in comparison with variance of slopes S_{xx}^2, as is the case for a knife beam. We can then rewrite Eq. (1) as

$$\sigma_{0y} = \frac{|R_{\rm eff}(U_{10})|^2}{2S_{xx}}\left(S_{yy}^2 + \frac{\delta_y^2}{5.52}\right)^{-1/2}. \tag{3}$$

Hence, we have a system of two equations [Eqs. (2) and (3)] and three unknown values: two variances of slopes and the effective reflection coefficient. After transformation, we obtain the following formula for the slope variance along the y axis:

$$S_{yy}^2 = \frac{\delta_y^2\sigma_{0y}^2}{5.52(\sigma_{00}^2 - \sigma_{0y}^2)}. \tag{4}$$

The rotation of the antenna system will allow us to measure the slopes along any direction, for example, along the x axis:

$$S_{xx}^2 = \frac{\delta_y^2\sigma_{0x}^2}{5.52(\sigma_{00}^2 - \sigma_{0x}^2)}, \tag{5}$$

where σ_{0x} is a radar cross section in the case of footprint orientation along the x axis.

From this, it is possible to determine the direction of wave propagation by using a rotating antenna system or by organizing a circular flight of the aircraft. The maximal value of NRCS will then correspond to the orientation of the footprint along the direction of wave propagation (Karaev et al. 2002b).

From Eqs. (2), (4), and (5), it follows that the effective reflection coefficient can be calculated using the retrieved variance of slopes [see Eq. (2)]:

$$|R_{\rm eff}(U_{10})|^2 = \sigma_{00}2S_{xx}S_{yy}. \tag{6}$$

As we see, we use the measurements of the normalized radar cross section by both a narrow-beam (σ_{00}) and a knifelike-beam (σ_{0y}) radar. However, it is not necessary to have two radars. The application of time selection allows us to select a scattering cell immediately beneath the radar (at nadir) and interpret this value as the NRCS of a radar with a narrow beam at nadir.

The effective reflection coefficient depends on the spectral density of small ripples (Elfouhaily et al. 1998). As a result, the direct measurement of the surface slope variance permits us to take into account the effect of surface slopes on nadir NRCS and makes the connection of radar cross section and the wind speed less ambiguous.

An airborne radar having a knifelike-beam antenna pattern ($1° \times 25°$) will successfully measure the direction of wave propagation, the variance of the surface wave slopes, and the wind speed. A difference occurs for a satellite-borne radar (flying at a height of ~800 km) for which the size of the footprint (~200–300 km) becomes larger than the spatial scale of ocean wave variability, and would result in strongly averaged measurements with all the information on phenomena at a smaller spatial scale being lost.

4. Application of time or Doppler selection for spaceborne knife-beam radar

As noted above, a satellite-borne radar (~800 km altitude) with an asymmetric knife beam will have a large footprint (~200–300 km). Let us see how we can improve the spatial resolution.

Let the knifelike-beam footprint and flight direction be oriented along the y axis (see Fig. 1). Here V is the velocity of the platform; θ_1, θ_2 are the incidence angles; R_1, R_2 are the slant ranges for two different scattering points along the y axis; and H_0 is the height of the platform.

Due to the narrow beamwidth across the footprint (1°), the across-track resolution will be of the order of

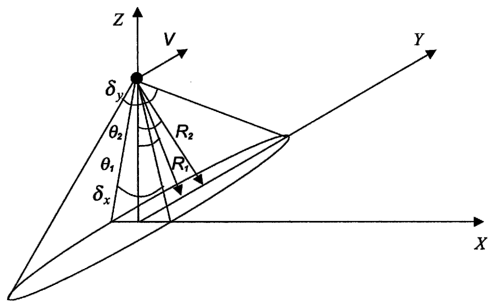

FIG. 1. Scheme of observation with an asymmetric knife-beam radar system.

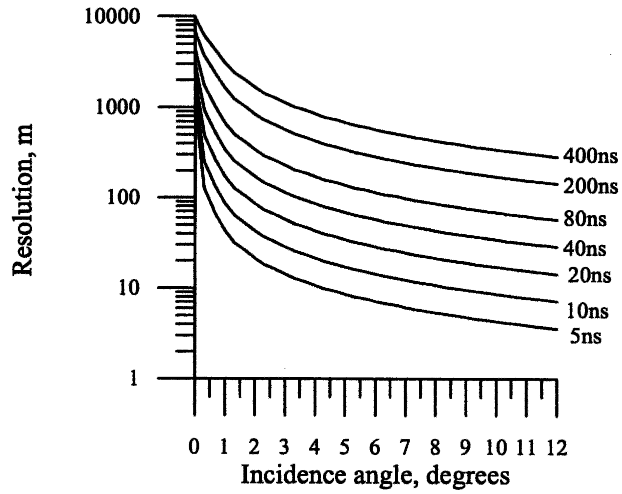

FIG. 2. Dependence of the range resolution on incidence angle for a few sample time steps (5, 10, 20, 40, 80, 200, 400 ns).

14 km, which is acceptable for wave studies. Clearly this value depends on the width of the radar beam and the height of the satellite. Our goal is to improve the resolution along the y axis (or direction of flight).

Conventional altimeters are pulse-limited systems designed to measure with high accuracy the time between the transmitted signal and the echo received from the ocean surface. Suppose at time $t = 0$, a radar pulse (the pulse width is T_{imp}) is emitted by the radar transmitter. At time $t = 2H_0/c$, the receiver will see the first return from the nadir point, the point on the surface closest to the altimeter. At any time $t > 2H_0/c$, the received power will come from points on a disk centered on nadir on the surface. The disk is the intersection of the spherical shell with the ocean surface. The return waveform will have three separate regions: 1) baseline (before the radiation reaches the surface); 2) leading edge, with power increasing linearly as a function of time (as the illuminated circle grows); 3) plateau, unless there are antenna gain drop-offs (Chelton et al. 1989).

Usually, to obtain a good range resolution, time selection is used. Let us introduce the sampling time step τ. Hence, the slant range for two successive scattering points in the footprint is $R_2 = R_1 + c\tau/2$, where c is the speed of electromagnetic waves. For such an observation scheme (see Fig. 1) the range resolution will be equal to $\Delta y = y_2 - y_1$, which after simple geometric considerations reads

$$\Delta y = H_0\left(\sqrt{\frac{[1 + c\tau\cos\theta_1/(2H_0)]^2}{\cos^2\theta_1} - 1} - \tan\theta_1\right). \tag{7}$$

The range resolution thus depends on the time sampling τ and the incidence angle θ_1. In Fig. 2, we show the dependence of the range resolution on incidence angle for a few values of the sampling time ($\tau = 5, 10, 20, 40, 80, 200, 400$ ns). We see that time selection gives good spatial resolution except the incidence angles less than 1°. It is therefore possible without too much effort to obtain a range resolution less than 10 m. For measurements of surface slopes such a small resolution is not required, however. On the contrary, small scattering cells would lead to large fluctuations in the reflected power due to the effects of individual waves, and additional averaging would be required.

For our purpose, the new radar must measure not only the power of the reflected signal but also its spectral characteristics. The Doppler shift of the reflected signal depends on the platform velocity and incidence angle and allows us to separate positive and negative velocities. Hence, the Doppler shift allows us to identify the reflected signals from the same range but from different sides of the radar. From this the normalized radar cross section can be calculated for every elementary cell inside the footprint.

Another approach for range selection is based on the use of Doppler selection. If the radar signal is backscattered by a target with relative velocity in respect to the radar, the signal will display a Doppler shift. We suggest dividing the Doppler spectrum of the reflected signal using a velocity/frequency filter. The power in every frequency channel gives us the reflected power from every elementary cell.

Due to the motion of the radar, the reflected signal will display a frequency shift with regard to the carrier frequency, which depends on the incidence angle and the velocity of the satellite. If ΔV is the width of the filter velocity, the formula for the range resolution with Doppler selection is

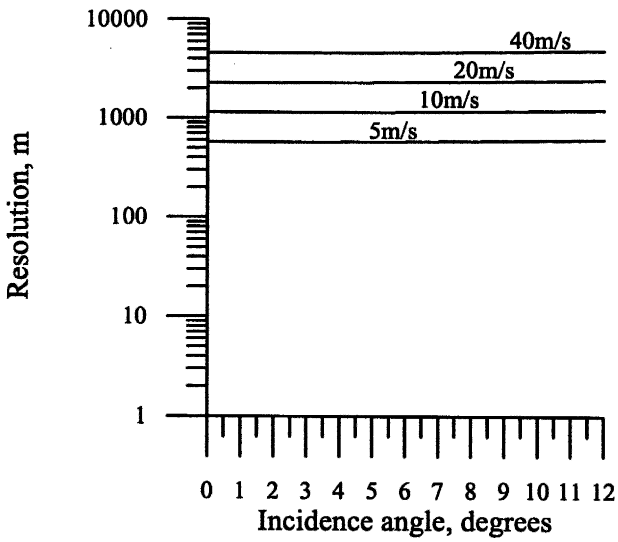

FIG. 3. Dependence of range resolution on incidence angle for a few Doppler velocity intervals ΔV (5, 10, 20, 40 m s^{-1}).

$$\Delta y = H_0\left(\frac{\sin\theta_1 + \Delta V/V}{\sqrt{1-(\sin\theta_1 + \Delta V/V)^2}} - \tan\theta_1\right). \quad (8)$$

Here we assume an azimuthally narrow radar beam ($\delta_x \approx 1^0$) and do not take into account any changes in azimuthal incidence angle within the antenna footprint. Figure 3 shows the dependence of the range resolution for Doppler selection on incidence angle for a few values of ΔV (ΔV = 5, 10, 20, 40 m s^{-1}).

In contrast to the time selection case, the Doppler selection gives a spatial resolution, which is practically independent of incidence angle. However, good spatial resolution (<500 m) can only be obtained for small value of ΔV (<5 m s^{-1}), in which case it is necessary to take into account the orbital velocity of the ocean surface. Hence, the movement of the sea surface (orbital velocity) does not allow us to achieve high resolution with Doppler selection. Such a limitation is absent for time selection. However, the resolution achievable with moderate value of ΔV (e.g., ΔV ~10 m s^{-1}) is sufficient for measurements of surface wave slopes (over a footprint of ~1 km). The resolution obtained with Doppler selection may be also useful for measurements over land for classification of land relief.

Therefore, the large asymmetric footprint (when seen from space, at a typical altitude of ~800 km) may be divided into elementary scattering cells as small as, for example, 14 km × 1 km or 14 km × 14 km. Indeed, the size of the elementary cells may be even smaller, although one should remember that decreasing the size of the cells would increase NRCS fluctuations and require successive averaging.

5. Doppler spectrum for radar with knife-beam antenna pattern

Let us consider the features of the Doppler spectrum of the backscattered microwave signal as applied to the problem of measuring the variance of surface slopes from a moving platform. For a stationary radar, the Doppler spectrum of the backscattered microwave signal contains more information about the ocean surface's characteristics than the normalized radar cross section (Bass and Fuks 1972), which is generally only an integral property of the surface and can be considered as one of the parameters of the Doppler spectrum.

The width of the Doppler spectrum is determined by the orbital velocities of the sea waves for a stationary radar. The motion of the radar leads to a loss of information in the Doppler spectrum about ocean surface. The Doppler spectrum becomes much wider, although the integral over the Doppler spectrum (normalized radar cross section) remains the same. Therefore, the normalized radar cross section is generally used for the remote sensing of the ocean, while Doppler radars are used on aircraft primarily to measure the flight velocity. This conventional view of Doppler spectrum is explained by the predominant use of radars with narrow antenna patterns.

Based on the method used to derive the knifelike-beam system's radar cross-section theoretical formulation (Karaev and Kanevsky 1998, 1999; Karaev et al. 2002b), a new theoretical model for the Doppler spectrum of a radar with a broad antenna pattern can be developed. For the case of nadir probing with a knife-like antenna pattern, with only minor approximation, we obtain the following formula for the width of the Doppler spectrum at the −10 dB level (Meshkov and Karaev 2004):

$$\Delta f_{10}[\mathrm{Hz}] = \frac{4\sqrt{2\ln 10}}{\lambda}\left[S_{tt}^2 - \frac{K_{xt}^2}{S_{xx}^2} - \frac{K_{yt}^2}{S_{yy}^2} + \frac{K_{xt}^2\delta_x^2}{S_{xx}^4(5.52 + \delta_x^2/S_{xx}^2)} + \frac{(V - K_{yt}/S_{yy}^2)^2\,\delta_y^2}{(5.52 + \delta_y^2/S_{yy}^2)}\right]^{1/2}, \quad (9)$$

where λ is the radar wavelength of the radar signal, S_{tt}^2 is variance of the vertical component of the orbital velocity, and K_{xt} and K_{yt} are two coefficients defined by the following formula:

$$K_{\alpha\beta} = 0.5\frac{\partial^2 K(\rho,\tau)}{\partial\alpha\partial\beta}\bigg|_{\rho,\tau=0},$$

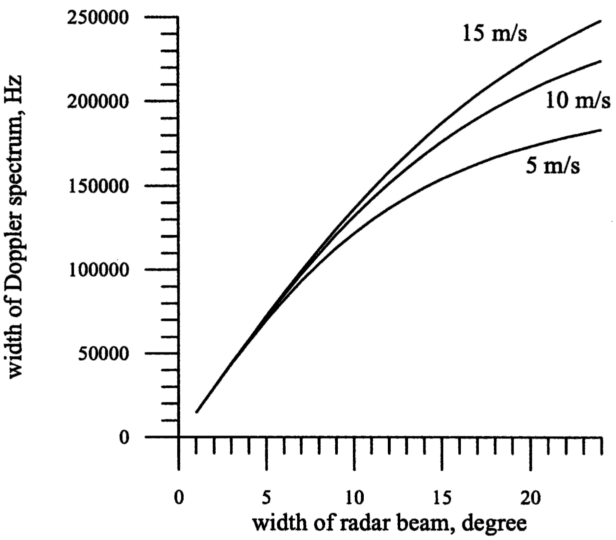

FIG. 4. Dependence of the width of the Doppler spectrum on antenna beamwidth for thee wind speeds (5, 10, 15 m s^{-1}). The platform velocity is 7000 m s^{-1}, and the direction of wave propagation is along the y axis.

where $K(\rho, \tau)$ is the correlation function of ocean surface heights (Bass and Fuks 1972).

Therefore, the Doppler spectrum for a stationary radar allows us to obtain information about the orbital velocity of the sea surface and thus estimate the dominant ocean wavelength. The motion of the radar makes this information inaccessible because the orbital velocity is significantly smaller than aircraft/spacecraft speed.

What are the novel aspects of these results? In Eq. (9) we correctly take into account the width of the antenna pattern, which shows us the new capabilities of the Doppler spectrum to resolve problems of remote sensing. It also shows that it is possible to measure surface wave slope variances from a moving radar using the Doppler spectrum information (Meshkov and Karaev 2001).

In Fig. 4, the dependence of the Doppler spectrum width on the antenna beamwidth is shown for three wind speeds (5, 10, 15 m s^{-1}), and a 7 km s^{-1} platform velocity (assuming an altitude of ~800 km). The antenna footprint is oriented along the y axis/flight direction (as in Fig. 1), as is the direction of wave propagation.

As discussed earlier, a radar with a narrow beam does not "see" the ocean surface, and the spectral characteristics of the reflected signal depend on the velocity of the platform up to a few degrees incidence. However, as the radar beamwidth increases, the difference between wind speeds becomes evident. In Fig. 4, the width of the Doppler spectrum for different wind speeds coincides for small antenna beamwidths. For antenna beamwidths larger than a few degrees, the reflected signals contain information about the sea surface in the Doppler spectrum and it becomes possible to retrieve the wave slope variance.

For increasing antenna beamwidths the growth of the Doppler spectrum is slower, as the area of intense specular reflection is not large and depends on the variance of slopes: the greater the range of incidence angles is within the footprint, the stronger the Doppler shift, but also the weaker the reflected signal. Therefore, at low wind speed (when the variance of slopes is small) "saturation" of the Doppler spectrum width is faster (Fig. 4). For a knifelike-beam antenna, the high velocity of the platform has a positive effect, increasing differences in the Doppler spectrum for different variances of slopes.

For an airborne radar, the signal would be processed and the Doppler spectrum calculated for the whole illuminated footprint. In the case of a spaceborne radar, the size of a footprint will be large in comparison with the length scale of most wave process variability on the ocean surface. Thus, to apply this approach to a satellite-based system, it is necessary to synthesize the Doppler spectrum as for the normalized radar cross section. This problem is considered in the next section.

To summarize, what are the advantages of extracting information from the Doppler spectrum instead of using the normalized radar cross section? Above we found that the width and frequency shift of the Doppler spectrum depend only on the properties of the large-scale waves. Therefore, environmental factors affecting small-scale waves (e.g., rain, surface films) do not affect the parameters of the Doppler spectrum. Hence, the combination of NRCS and Doppler spectrum information is a promising approach to obtain new oceanographic observations by remote sensing.

6. The first look at measurements and data synthesis

Let us return to the problem of the size of elementary scattering cell. For a knifelike-beam antenna radar, the antenna beamwidth across the footprint, δ_x, determines the azimuth resolution. The spatial resolution is then given approximately as $H_0 \tan\delta_x/\cos\theta_1$.

The spatial resolution in range may be based on either time or the Doppler selection (see section 3). Evidently, the size of the scattering cell must allow us to retrieve the information about wave processes on the ocean surface. It is possible to obtain very good range resolution using time selection. However, high spatial resolution leads to large fluctuations in the power of the

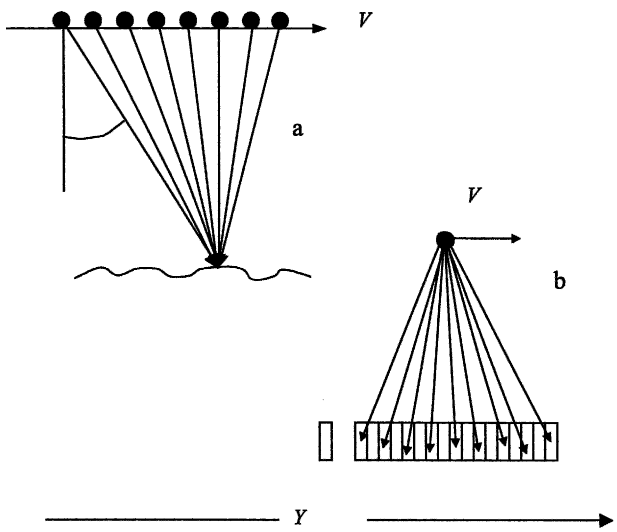

FIG. 5. Transformation of one cell in footprint (synthetic procedure).

reflected signal. On the other hand, it is always possible to degrade the resolution and reduce fluctuations by either increasing the size of individual cells or summing over a number of cells. Also, it is necessary to take into account the technical aspect of this question, that is, how much data from how many scattering cells it is possible to record during the flight.

If we intend to measure the surface wave slopes and to detect the effect of currents, storms, and other processes on the ocean surface, the range resolution may need to be as small as a few hundred meters. Therefore, we can apply both time selection and Doppler selection.

The next question is, how should we process and synthesize the data? The big advantage of a knife-beam antenna, in comparison with a nadir-looking narrow-beam radar is that we observe all scattering cells for a range of incidence angles, for example, from $-10°$ to $10°$ if $\delta_y = 20°$. As a result, we measure both the distribution of slope along the y axis and the variance of surface wave slopes. For a radar with a knife-beam antenna pattern we can apply a special synthesis procedure to process the data. Let us see what this synthesis procedure entails.

Let the radar fly over the ocean surface (Fig. 1). The footprint may be divided into elementary scattering cells, for example, 14 km $\times$ 14 km. A wide antenna pattern along the direction of flight allows us to observe the elementary cell at different incidence angles.

Let us choose some scattering cell for further consideration. During flight, the radar will see this cell under a range of incidence angles (see Fig. 5a). As a result we will measure the dependence of the reflected power on the incidence angle for that scattering cell. As the wave profile is skewed, the dependence will be skewed too. Hence, it is possible to measure the skewness of ocean waves in the flight direction.

Collecting all the data about this cell (different incidence angles/different times), we may interpret our observations in the following way: the radar simultaneously sees the scattering area (footprint) with its wide beam (see Fig. 5b). The difference between elementary "cells" in this footprint is a time difference. The existence of this difference is very useful: we may choose uncorrelated "cells." For example, for $H_0 = 800$ km, $\delta_x = 20^0$, $V = 7$ km s^{-1}, a given point can be observed within the antenna footprint for 40 s. Since the decorrelation time of the ocean surface is approximately 0.1 s (Winebrenner and Hasselmann 1988), we can obtain 400 independent measurements during the observation interval, assuming continuous observation. Therefore, the noise level is small.

Such a synthesis procedure permits significant improvement in the spatial resolution. Instead of dealing with a whole footprint (e.g., ~14 km $\times$ ~280 km) we can work with individual scattering cells (e.g., 14 km $\times$ 14 km). With such an approach, the resolution is good and we can apply Eq. (1) to the spaceborne radar and measure the variance of surface wave slopes in every elementary cell.

We may define the radar cross section for each cell σ_{0yi} by summing up all radar cross sections σ_j for that cell at different times/incidence angles ($j = 1, \ldots, N$), where N is the total number of observations of that cell, in the hypothetical case of sea waves homogeneous inside the entire footprint (see Fig. 5b):

$$\sigma_{0yi} = \frac{1}{N}\sum_{i=1}^{N} \sigma_j, \tag{10}$$

where σ_j is the radar cross section of the jth scattering cell at an incidence angle θj inside of footprint (the index j may be also interpreted as different times of observation). Hence, the value σ_{00}, needed to calculate slope variances (4), is obtained as the σ_{0yj} value for the cell located immediately under the radar.

The measured value of slope variance can be used for the development of new algorithms for wind speed retrieval, as previously suggested.

7. Numerical simulation

In our previous studies we have developed numerical simulations of the ocean surface and of the response of radar systems (Karaev et al. 2000a,b; see the brief summary of simulation approach in the appendix herein). It is a quick and affordable way to validate the conclusions of the theoretical results, to determine the optimal characteristics of radar, and to estimate the precision of retrieval algorithms.

Although our goal is to develop and validate the concept of a new radar for space implementation, we have not been able to numerically simulate a spaceborne system. For this a powerful computer is required, so we will only show results for a platform traveling at low velocity and height (as in the case of aircraft).

Let a knifelike-beam radar carrier fly along the y axis (Fig. 1). Then the following parameters are used for calculations unless specified otherwise: height of flight is 5 km, velocity is 300 m s^{-1}, antenna beamwidths are $1° \times 20°$, and the orientation of the footprint is along the flight direction. The reflected signal is averaged over 10 samples, the repetition frequency is 0.1 Hz, and the pulse width is 100 ns.

a. Antenna beamwidth

In Fig. 6, the reflected pulse waveforms are shown. The power of the backscattered signal increases with time until the back edge of the incident impulse reaches the surface. The calculations have been made for the following values of antenna beamwidths δ_y = 5°, 10°, 20°, 40°. At narrow radar beamwidths we see a plateau, which is absent for a wide-beam radar. For a wide beam, after the maximum value is reached the power of the reflected signal begins to decrease. From the slope of the leading edge of the pulse, it is possible to recover SWH for information, as for conventional altimeters.

The main weakness of the wide-beam configuration is the large transmitted power required. An initial estimate suggests that the power of the radar will need to be 30–50 times larger than for altimeters with a narrow beam (say $1° \times 1°$). This is due to the large footprint of the system.

b. Platform height

The dependence of the waveform on the height of flight is shown in Fig. 7. The calculations were carried out for heights of 5, 20, and 50 km. The increase in flight height leads to an increase in the length of the returned echo. Therefore, there exists a limit for the pulse repetition frequency related to this echo broadening. Assume the height above the sea surface to be 800 km and the width of the antenna pattern to be 25°. In this case, the length of the reflected pulse will be equal to the length of the emitted pulse plus pulse broadening, estimated to be ~130 μm. Therefore, the frequency of repetition must be high enough, for example a few kilohertz, to allow the calculation of the Doppler spectrum with good frequency resolution.

c. Pulse width

One of the most important parameters of a radar is its pulse width. In Fig. 8, the dependence of the re-

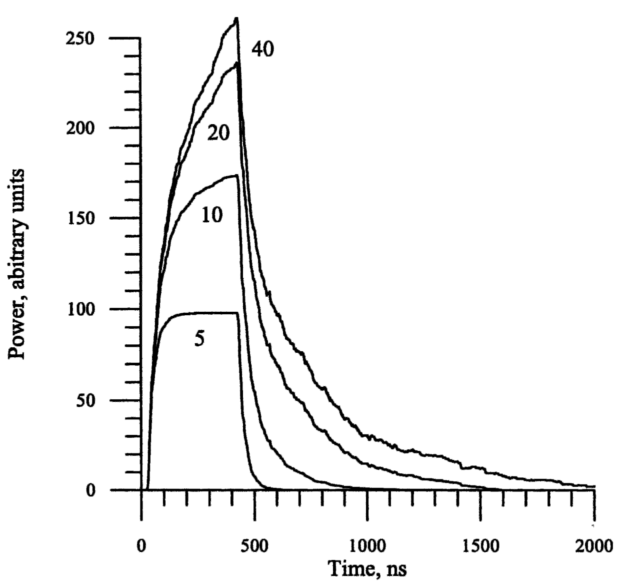

FIG. 6. Received power as a function of time for different antenna beamwidths. The calculations were performed for a height of flight of 5 km, a wind speed of 10 m s^{-1}, and a pulse width of 400 ns.

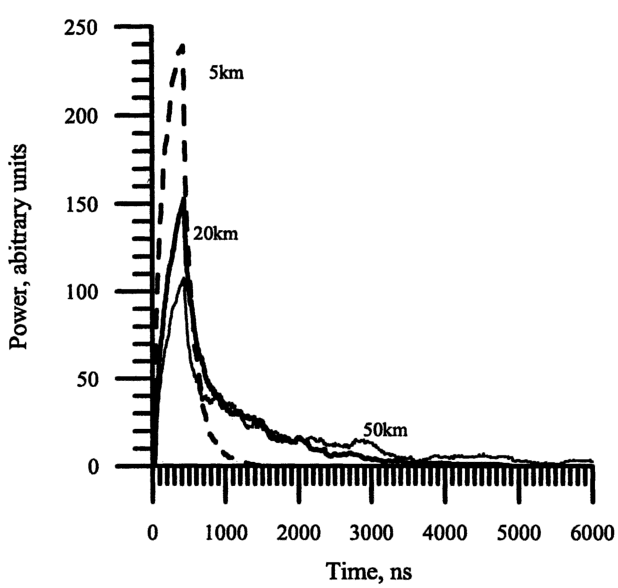

FIG. 7. Dependence of reflected power on time for various platform flight heights: 5, 20, and 50 km. The pulse width is 400 ns, and the wind speed is 10 m s^{-1}.

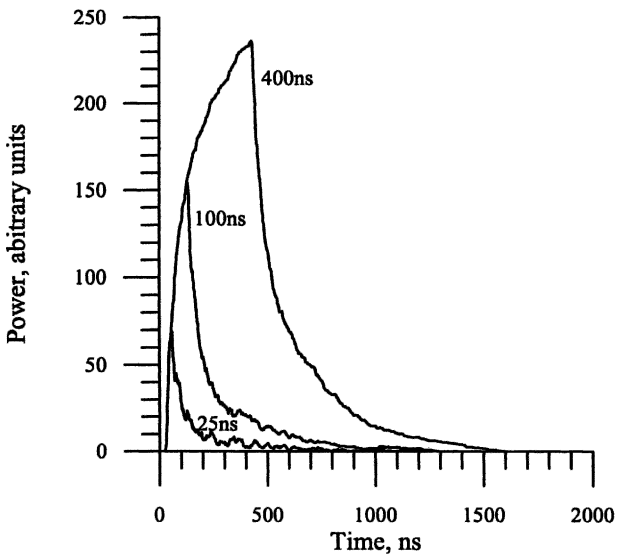

FIG. 8. Examples of waveforms for different pulse widths: 25, 100, 400 ns. The height is 5 km, the wind speed is 10 m s^{-1}, and the beamwidth is 1° × 20°.

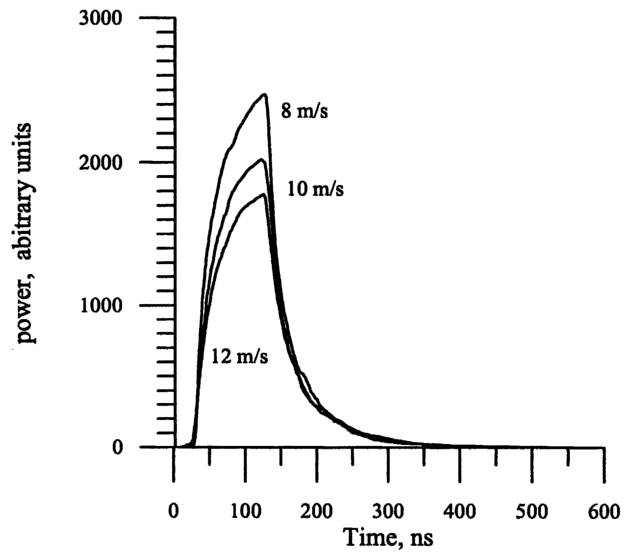

FIG. 9. Dependence of waveforms on wind speed for fully developed wind waves. The pulse width is 100 ns, the height is 1 km, and the direction of wave propagation is along the y axis.

flected power is shown against time of delay for a few values of the pulse width: 25, 100, 400 ns. The pulse width determines the maximal area of ocean illuminated simultaneously. For the calculations, the wind speed was equal to 10 m s^{-1}, the radar beamwidth being 20°. Increasing the pulse width leads to an increase in the maximum value of waveform and reduces the fluctuations of reflected signal due to the effect of averaging over the pulse width.

d. Sea state

The main objective of a new radar concept is the measurement of new characteristics of the ocean surface. Therefore, we have calculated the waveforms for different ocean states. In Fig. 9 the dependence of the waveforms on wind speed is shown. We see that the radar is sensitive to the ocean state, with increasing wind speed leading to decreasing reflected power.

8. Example of data processing

In our research we mainly aim to develop new methods to measure other sea state parameters. In the previous sections the design of the radar has been discussed and numerical simulations of the backscattered signal have been carried out. We next look at the data processing of the reflected signal.

Let us consider the next processing of the reflected pulse using, for example, Doppler selection. The waveform is shown in Fig. 10a. The simulations are carried out for a height of flight of 1 km, a pulse width of 100 ns, and a platform velocity of 300 m s^{-1}. The averaging is performed over 20 pulses, the pulse repetition frequency is 0.1 Hz, and the wind speed is 10 m s^{-1}. For such a pulse (see Fig. 10) the corresponding Doppler spectrum is as shown in Fig. 10b.

The Doppler spectrum represents possible Doppler velocities present in the reflected signal. If we divide the Doppler velocities axis into 20 intervals and calculate the power of the reflected signal in each interval/cell, we perform spatial sampling using Doppler selection. Figure 11 shows the distribution of power in cells/angles. In the case of experimental measurements, the asymmetry of this power profile, essentially the dependence of the reflected power on incidence angle, will provide a measure of the asymmetry of the wave profile in the footprint.

We can then apply the method developed earlier [Eq. (4)] to calculate the variance of the surface slopes in the footprint. As a result we obtain a variance of surface slopes along the direction of flight as $S_{yy}^2 =$ 0.0182, which compares favorably with the true value of 0.0189 derived from the wave spectrum used in the simulation. The explanation of the small difference is the poor spatial and temporal averaging chosen in order to speed up the numerical calculations.

9. Conclusions

The present work continues our research on electromagnetic scattering from the sea surface at small inci-

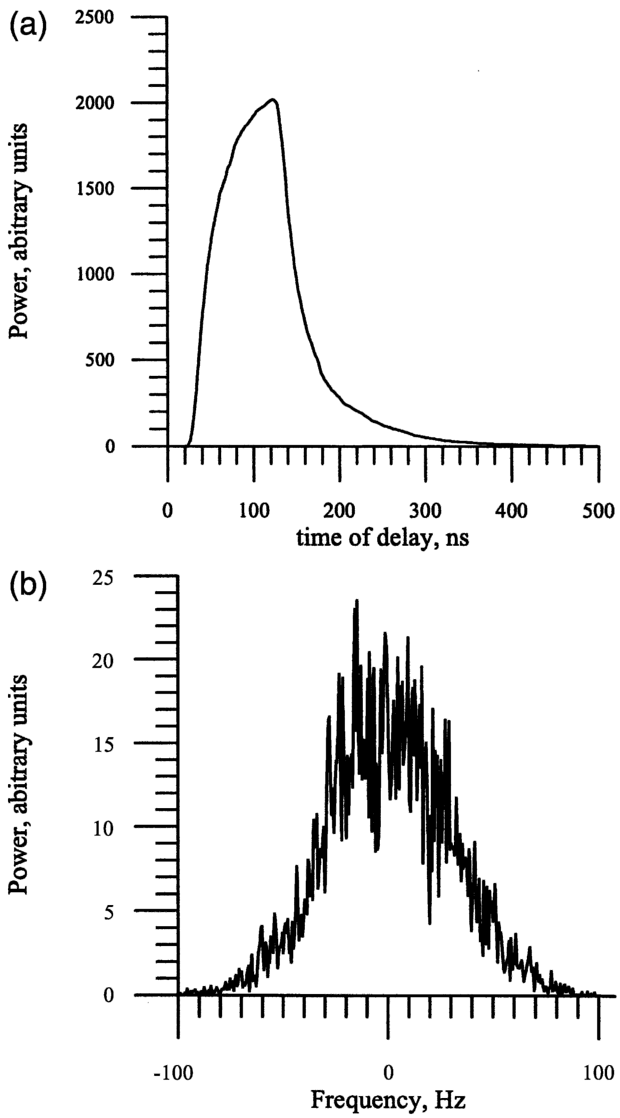

FIG. 10. (a) Power received as a function of time. The wind speed is 10 m s^{-1}. (b) Doppler spectrum of backscattered signal seen in (a). Radar velocity is 300 m s^{-1}, and the wind speed is 10 m s^{-1}.

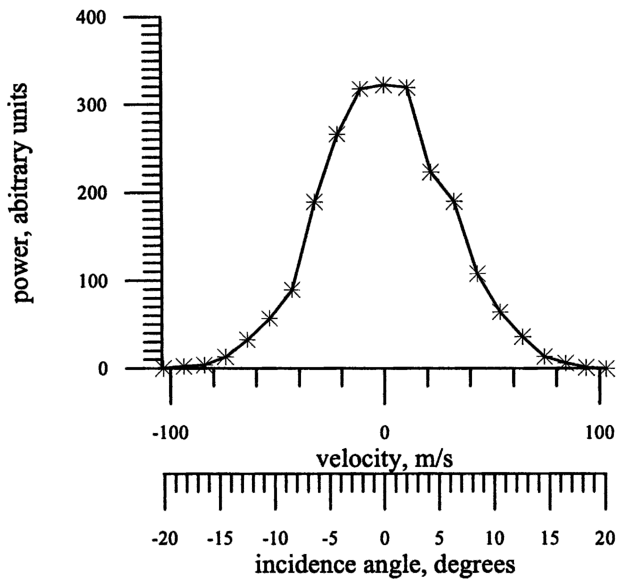

FIG. 11. Dependence of reflected power on incidence angles as obtained from the Doppler spectrum shown in Fig. 10b.

dence angles as applied to ocean remote sensing. The simple configuration of a Doppler radar with a knife-beam antenna pattern oriented along flight direction has been discussed.

The analysis has been based on new theoretical models for the radar cross section and the Doppler spectrum of radar with a wide antenna pattern in one direction. The new radar concept is viable when installed on aircraft but encounters a major problem for spaceborne implementation due to the large size of the footprint. We have suggested solving the problem by range selection and subsequent data processing. Two types of range selection based either on time or on Doppler selection have been discussed.

The great advantage of a knife-beam antenna, in comparison with a narrow radar beam, is that each scattering cell is observed at all incidence angles within the beam, for example from $-10°$ to $10°$. Thus, a simple radar with a knifelike antenna pattern can make direct measurements not only of the significant wave height (SWH) but also of the surface wave slopes. Comparing the reflected power measured at the same range but different by the sign of the Doppler shift makes it possible to obtain a measure of the asymmetry of the wave profile.

The numerical simulations (though limited by computational resources) confirmed our theoretical results and allowed the investigation of the properties of the new system for various radar and ocean parameters. This has helped to determine the optimal characteristics of the radar system at this first stage of the development.

Thus, the new radar will allow us to measure new ocean parameters such as the long-wave slopes and will help increase the precision of wind speed retrieval with conventional nadir altimeter. Further sea state parameters may be retrievable if one considers an advanced version the knifelike-beam radar with a rotating antenna (here the knife beam is aligned in the flight direction and kept fixed). As a result, the rotating radar knifelike beam would collect information in a wide swath configuration. The properties of this rotating antenna system will be considered later.

Acknowledgments. This work was supported by the Russian Foundation of Basic Research (Project N 03-05-64259).

APPENDIX

The Numerical Simulations

A standard Gaussian statistical model of waves at the sea surface is used for the numerical simulations (Longuet-Higgins 1962). The simulated sea surface elevation Σ is represented as a superposition of sinusoidal waves with different frequencies ω_n and random phase ψ_{nm}, propagating at different azimuthal angles φ_m:

$$\Sigma(\mathbf{r}, t) = \sum_{n=1}^{N} \sum_{m=1}^{M} A_n \cos(\omega_n t + \mathbf{k}_n \mathbf{r} + \psi_{nm}) \Phi_{nm}(\omega_n, \varphi_m),$$

where ψ_{nm} is a random phase uniformly distributed on 0 to 2π. Here the wavenumber κ and frequency ω_n are related via the dispersion relationship. The amplitude of nth harmonic A_n is the power in an interval $\Delta\omega_n$ and is calculated from the wave frequency spectrum $S_\sigma(\omega)$:

$$A_n = \sqrt{2\Delta\omega_n S_\sigma(\omega_n)}.$$

The coefficients Φ_{nm} determine the azimuthal distribution of wave spectrum and are calculated from the following formula:

$$\Phi_{nm}(\omega_n, \varphi_m) = \sqrt{\Phi_\omega(\omega_n, \varphi_m)\Delta\varphi},$$

where Φ_ω describes the angular spread of wave spectrum, and $\Delta\varphi$ is uniform increment in the azimuthal angle. For the numerical simulation we used only large-scale waves in comparison with the radar wavelength (in the framework of the two-scale model). The model of wave spectrum used in calculations was that of Karaev et al. (2000b).

This algorithm was implemented numerically. The simulated surface was then illuminated by a radar with a knife-beam antenna pattern. The program calculates the emitted field (transmitted pulse), finds the reflection points on the simulated sea surface, and determines the reflected pulse, taking into account the slant distance, the velocity of radar, the orbital velocity of sea waves, and the radar antenna pattern. We use the Kirchoff approximation and therefore assume that facets of the wave profile that are perpendicular to incident field are the reflection points.

A problematic issue with the numerical simulation is the restriction on the height, at which the radar is to be flown, that can be simulated. Unfortunately, the time taken to carry out a single simulation for a radar altitude of 500–800 km, typical of spaceborne systems, is prohibitive. Even for a radar at a height of 50 km it takes 2 weeks of the computer time available to us for a simulation involving a single set of parameters. Since it is necessary to be able to simulate a variety of sea states and radar system characteristics, we have therefore simulated a radar system for very "low orbits" (i.e., simulating an airborne rather than a spaceborne radar).

For more details of this approach and its numerical implementation the reader is referred to Karaev et al. (2000a,b).

REFERENCES

Barrick, D. E., 1972: First order theory and analysis of MF/HF/VHF scatter from the sea. *IEEE Trans.,* **AP-20,** 2–10.

Bass, F. G., and I. M. Fuks, 1972: *Scattering of Waves by the Statistically Rough Surface* (in Russian). Nauka, 424 pp.

Chelton, D. B., E. J. Walsh, and J. L. MacArthur, 1989: Pulse compression and sea level tracking in satellite altimetry. *J. Atmos. Oceanic Technol.,* **6,** 407–438.

Elfouhaily, T., D. Vandemark, J. Gourrion, and B. Chapron, 1998: Estimation of wind stress using dual-frequency Topex/Poseidon data. *J. Geophys. Res.,* **103,** 25 107–25 108.

Gommenginger, C. P., M. A. Srokosz, P. G. Challenor, and P. D. Cotton, 2002: Development and validation of altimeter wind speed algorithms using an extended collocated buoy/Topex dataset. *IEEE Trans. Geosci. Remote Sens.,* **40,** 251–260.

Gourrion, J., D. Vandemark, S. Bailey, and B. Chapron, 2000: Satellite altimeter models for surface wind speed developed using ocean satellite crossovers. Tech. Rep. N IFREMER-DROOS-2000-2, 69 pp.

Hauser, D. G., G. Caudal, G. J. Rijckenberg, D. Vidal-Madjar, G. Laurent, and P. Lancelin, 1992: RESSAS: A new airborne FM/CW radar ocean wave spectrometer. *IEEE Trans. Geosci. Remote Sens.,* **30,** 981–995.

——, E. Soussi, E. Thouvenot, and L. Rey, 2001: SWIMSAT: A real-aperture radar to measure directional spectra of ocean waves from space—Main characteristics and performance simulation. *J. Atmos. Oceanic Technol.,* **18,** 421–437.

Hwang, D. A., and O. H. Shemdin, 1988: The dependence of the sea surface slope on atmospheric stability and swell conditions. *J. Geophys. Res.,* **93** (C11), 13 903–13 912.

Karaev, V. Yu., and M. B. Kanevsky, 1998: Development of the remote sensing methods: Measurement of the ocean surface tilts by microwave radar. *Proc. Fourth Pacific Ocean Remote Sensing Conf. (PORSEC '98)*, Quigdao, China, Pacific Ocean Remote Sensing Congress, 387–390.

——, and ——, 1999: On the problem of the radar determination of the sea surface parameters (in Russian). *Issled. Zemli Kosm.,* **4,** 14–21.

——, ——, P. D. Cotton, P. G. Challenor, C. Gommenginger, and M. Srokosz, 1999: Two-parametric algorithm of the wind speed retrieval by altimeter data. *TOPEX/POSEIDON and Jason-1 Science Working Team Meeting*, Saint Raphael, France, NASA/CNES, 80.

——, ——, and G. N. Balandina, 2000a: The numeral simulation of the sea surface and remote sensing (in Russian). Institute of Applied Physics, Nizhny Novgorod, Russia.

——, ——, and ——, 2000b: A modified wave spectrum and remote sensing of ocean (in Russian). *Issled. Zemli Kosm.,* **5,** 1–12.

——, ——, ——, P. D. Cotton, P. G. Challenor, C. P. Gommenginger, and M. A. Srokosz, 2002a: On the problem of the near ocean surface wind speed retrieval by radar altimeter: Two-parameter algorithm. *Int. J. Remote Sens.,* **23,** 3263–3283.

——, ——, P. D. Cotton, and P. G. Challenor, 2002b: Is it possible to measure ocean surface slopes with a microwave radar? *Int. J. Remote Sens.,* **23,** 3251–3262.

Lin, C., B. Rommen, J. J. W. Wilson, F. Impagnatiello, and P. S. Park, 2000: An analysis of a rotating, range-gated, fanbeam spaceborne scatterometer concept. *IEEE Trans. Geosci. Remote Sens.,* **38,** 2114–2121.

Longuet-Higgins, M. C., 1962: Statistical analysis of random moving surface. *Wind Waves* (in Russian), Yu. Krylov, Ed., Inostrannaya Literatura, 112–130.

Meshkov, E. M., and V. Yu. Karaev, 2001: The features of Doppler spectrum of microwave signal backscattered by see surface at small incidence angles (in Russian*).* Institute of Applied Physics, Nizhny Novgorod, Russia.

——, and ——, 2004: Determination of the parameters of sea surface roughness using the Doppler spectrum of a microwave radar signal reflected from a water surface. *Radiophys. Quant. Electron.,* **47,** 205–217.

Moccia, A., N. Chiacchio, and A. Capone, 2000: Spaceborne bistatic synthetic aperture radar for remote sensing applications. *Int. J. Remote Sens.,* **21,** 3395–3414.

Valenzuela, G. R., 1978: Theories for the interaction of electromagnetic and oceanic waves—A review. *Bound.-Layer Meteor.,* **13,** 61–86.

Walsh, E. J., D. W. Hancock III, and D. E. Hines, 1985: Directional wave spectra measured with the surface contour radar. *J. Phys. Oceanogr.,* **15,** 566–592.

Walsh, J. E., and D. C. Vandemark, 1998: Measuring sea surface mean square slope with a 36-GHz scanning radar altimeter. *J. Geophys. Res.,* **103** (C6), 12 587–12 601.

Winebrenner, D. P., and K. Hasselmann, 1988: Specular point scattering contribution to the mean synthetic aperture radar image of the ocean. *J. Geophys. Res.,* **93** (C8), 9281–9294.